Acta Biochim Biophys Sin (2010): 80–89 | © The Author 2009. Published by ABBS Editorial Office in association with Oxford University Press on behalf of the Institute of Biochemistry and Cell Biology, Shanghai Institutes for Biological Sciences, Chinese Academy of Sciences. DOI: 10.1093/abbs/gmp104.
Advance Access Publication 14 December 2009

Apoptotic mechanism of MCF-7 breast cells *in vivo* and *in vitro* induced by photodynamic therapy with C-phycocyanin

Bing Li[1]*, Xianming Chu[2], Meihua Gao[1], and Wuxiu Li[3]

[1]Department of Biology, Medical College of Qingdao University, Qingdao 266021, China
[2]Department of Cardiology, Affiliated Hospital of Medical College of Qingdao University, Qingdao 266000, China
[3]Shandong University of Science and Technology, Qingdao 265102, China
*Correspondence address. Tel: +86-532-82991208; Fax: +86-532-85953236; E-mail: libing_516@yahoo.com.cn

The aim of this study was to investigate the pro-apoptotic mechanism of C-phycocyanin (C-PC)-mediated photodynamic therapy (PDT) in a murine tumor model and cultured MCF-7 cells. The mice were divided into four groups: control, He–Ne laser radiation, C-PC treatment, and C-PC treatment + He–Ne laser radiation. The effects of C-PC and/or laser on immune organs, immunocyte proliferation, tumor genesis, and apoptosis-related proteins expressions were investigated by immunohistochemistry, *in situ* hybridization, MTT, electron microscope, western blot, and immunofluorescence assay. The results showed that He–Ne laser treatment alone showed marginal effects. In C-PC-treated mice, the weight of immune organs, proliferation of immunocytes, and expression of pro-apoptotic Fas protein were increased, whereas the tumor weight and the expressions of anti-apoptotic proteins (NF-κB and P53) and *CD44* mRNA were comparatively decreased. In *vitro*, C-PC was able to inhibit MCF-7 cell proliferation and cause ultrastructural changes including microvilli loss, formation of membrane blebs, and chromatin condensation. Moreover, C-PC treatment could activate caspase-9 expression, induce cytochrome c release, and downregulate Bcl-2 expression. When combined with He–Ne laser irradiation, the effects of C-PC treatment were further enhanced. Facilitating the apoptosis signals transduction and finally leading to the apoptosis of MCF-7 cells may be the mechanism of the anti-tumor activities of C-PC-mediated PDT.

Keywords apoptosis; C-phycocyanin; MCF-7 cells; He–Ne laser; PDT; anti-tumor effect

Received: June 17, 2009 Accepted: October 9, 2009

Introduction

It has been more than 30 years since photodynamic therapy (PDT) was developed as a useful and promising treatment tool in oncology. The approach has been used clinically for treating early or localized diseases and for improving the quality of life and increasing survival rate of patients with advanced diseases [1]. PDT involves localization of light-sensitive drugs (photosensitizer) in the target tissues prior to radiation with an appropriate wavelength [2]. Cytotoxic agents generated upon radiation trigger a cascade of biochemical responses that inactivate cancer cells either directly or through the induction of vascular stasis. PDT has an advanced, efficient, convenient system of light delivery as well as several potential advantages over surgery and radiotherapy. It is comparatively non-invasive and can be targeted accurately. Repeated doses can be given without total-dose limitation. The healing process rarely results in scarring. PDT is better tolerated as the treatment destroys diseased tissue while leaving normal tissue intact with no side effects [3]. The hematoporphyrin derivative, photofrin (R), has been approved to be one of the first-generation photosensitizers and used in the treatment of cervical cancer. Unfortunately, it has several disadvantages [4]. In order to enhance the potential of PDT and explore its application in other circumstances, currently, second-generation photosensitizers are being extensively investigated, which should be tumor localizing, non-toxic and absorbed in the red region of the spectrum.

C-phycocyanin (C-PC) is one of the major water-soluble biliprotein present in *Spirulina platensis* and the structure is similar to hematoporphyrin. This protein is frequently used in food products and in cosmetics because of its blue color and its strong fluorescence in the visible region. Recently, C-PC has been reported to have several biological activities including anti-tumor [5], hepatoprotective [6], anti-oxidant [7], radical scavenging [8], and anti-inflammatory functions [9]. Studies have revealed that C-PC significantly reduced the viability of mouse myeloma cells after radiation at dose of 300 J/cm^2 at 514 nm for 3 days compared with cells exposed to laser or phycocyanin only [5].

He–Ne laser (wavelength: 632.8 nm) is characterized by good directivity, high intensity, and good monochromaticity [10–13]. In addition, He–Ne laser has several other biological effects such as increasing cell vitality [14–16], improving phagocytosis [17–19], and promoting immune responses [20–23]. External radiation is easy, and patients can bear radiation-induced pain. So far, there are few reports concerning the application of He–Ne laser in the treatment of cancer [24–26].

To our knowledge, there are few researches currently focusing on the molecular mechanism of MCF-7 cell apoptosis induced by C-PC-mediated PDT. The present study was carried out to investigate the effects of C-PC on MCF-7 cells in combination with He–Ne laser both in a murine tumor model and in cultured cells. Possible mechanisms of apoptosis of MCF-7 breast cells induced by C-PC-mediated PDT were explored.

Materials and Methods

Materials

C-PC was extracted from *S. platensis* and purified as previously reported [27]. The purity of C-PC was 4.71 as shown by the ratio of A620/A280 nm. MCF-7 cell line was obtained from the Laboratory of Algal Biotechnology (College of Marine Life Sciences, Ocean University of China, Qingdao, China). BALB/c mice were purchased from Experimental Animal Center, Medical College of Qingdao University. Fas immunohistochemistry kit, CD44 *in situ* hybridization kit, and rabbit anti-human Fas/NF-κB/P53/Bcl-2/caspase-9 monoclonal antibodies were purchased from Boster Biological Engineering Co., Ltd (Wuhan, China). FITC-goat anti-human cytochrome c McAb was purchased from Invitrogen (Carlsbad, USA). Phosphate-buffered saline (PBS), RPMI 1640 medium, fetal bovine serum were purchased from Gibco (Pascagoula, USA). Poly-lysine and MTT [3-(4,5-dimethylthiazol-2-yl)-2,5-diphenyl tetrazolium bromide] were from Sigma (St Louis, USA).

Establishment of animal model and grouping

A total of 56 adult BALB/c mice (28 males and 28 females, weighing 20–22 g) were used for the study. The mouse tumor models were set up by subcutaneous injection of 1×10^5 MCF-7 cells near the spleen area. Twenty-four hours later, the mice were randomly divided into four groups: control group (16 mice), He–Ne laser radiation group (16 mice), C-PC treatment group (14 mice) which was given 2 ml C-PC (320 mg/ml), and C-PC + laser radiation group (10 mice) receiving 2 ml C-PC (320 mg/ml) followed 2 h later by He–Ne laser radiation. The animals were held by rat holders during He–Ne laser treatment. He–Ne laser was amplified by convex lens and vertically radiated at the splenic projective area. The anterioposterior diameter of laser was 0.5 cm. He–Ne laser therapy (wavelength: 632.8 nm, power density: 76.43 J/cm^2, output power: 24 mW/cm^2) was carried out once per day for 13 days, 10 min each time [28].

Collection of samples

After 13 days of treatment, the mice in each group were sacrificed by cervical dislocation at the desired time point and the celiac cavity was opened immediately. Thymus and spleen were taken out, and the tumor mass was separated from skin. The middle part of the tumor mass was cut into small pieces of $\sim 1.0 \times 0.5 \times 0.5$ cm^3 for preparing paraffin blocks. The remaining parts were triturated to make unicellular suspension.

Tumor weight and tumor forming rate

The average tumors were weighed and the tumor forming rates were calculated. Tumor forming rate was defined as the number of mice with tumor formation against the total number of mice in the each experimental group.

Determination of immunocyte proliferation ability by MTT assay

Thymocytes and splenocytes (5×10^6 cells/well) were cultured, respectively, in 96-well plates at 37°C in the presence of 20 μl of ConA (25 μg/ml) for 48 h in a final volume of 100 μl. Then, 10 μl of MTT (5 mg/ml) was added to each well. The mixture was incubated for an additional 5 h in 5% CO_2 at 37°C and then centrifuged at 112.5 *g* at 4°C for 10 min, and the supernatant was discarded. The precipitate was dissolved in 100 μl of DMSO and the absorbance values at 490 nm (A490 nm) were measured. The inhibition ratio of each group was calculated as follows: inhibition ratio = (A490 nm of control group − A490 nm of experiment group)/A490 nm of control group.

Immunohistochemistry staining

The paraffin slices were put on microscope slides previously coated with 0.1% poly-lysine solution. The slices were conventionally dewaxed and treated with 30% H_2O_2: methanol (1: 50) at room temperature for 5–10 min. After wash with distilled water, antigen was restored by heat. The expressions of proteins (Fas/NF-κB/P53) were examined by immunohistochemical staining. Briefly, after culturing in blocking buffer (provided in the immunohistochemistry kit), the slides were incubated with biotinylated rabbit anti-human Fas/NF-κB/P53 monoclonal antibodies, respectively (1:30, 1:100, 1:60), followed by incubation with streptavidin–biotin complex (SABC) and diaminobenzidine (DAB, for color development). The slides were observed under light microscope. The positively stained cells were counted in five randomly selected high power fields (×400), and the positive rate was scored as

following: <5%, 0 score; 5–25%, 1 score; 26–50%, 2 scores; 51–75%, 3 scores; 76–100%, 4 scores. An additional scoring system was applied based on coloration intensity: no coloration, 0 score; light coloration, 1 score; medium coloration, 2 scores; deep coloration, 3 scores.

The relative quantity of protein expression was determined on the basis of the combination of the two scoring systems employed: (−): 0–1 score, negative; (+): 2–3 scores, slightly positive; (++): 4–5 scores, moderately positive; (+++): 6–7 scores, strongly positive.

Screening *CD44* mRNA expression by *in situ* hybridization

Three oligonucleotide probes for *CD44* mRNA (30 bp labeled with digoxin at 5′ end) were synthesized by Boster Biological Engineering Co., Ltd (5′-GCAGATCGATTT-GAATATAACCTGCCGCTA-3′, 5′-TGAGCAGCGGCT-CCTCCAGTGAGAAGAGCA-3′, 5′-ACTCCAGAC CAG-TTTATGACAGCTGATGAG-3′). Cells were placed on microscope slides coated with 0.1% poly-lysine solution and fixed at room temperature for 20–30 min by 4% polyformadehyde/0.1 M PBS. After being washed with distilled water, the slides were treated with 30% H_2O_2: methanol (1:50) at room temperature for 30 min to block endogenous peroxidase activities and then washed with distilled water. Prehybridization was performed by adding 20 μl prehybridizational solution (provided in the CD44 *in situ* hybridization kit) on the slides and incubated in wet box at 38–42°C for 2–4 h. Then, 40 μl of hybridization liquid containing 40 ng probe was added on the slides which were then incubated overnight and washed with saline sodium citrate. *CD44* mRNA expression was determined by immunohistochemical staining. In brief, the slides were incubated in blocking buffer followed by incubation with biotinylated mouse anti-digoxin IgG, SABC, and DAB. The slides were observed under light microscope.

MCF-7 cell viability determined by MTT assay

MCF-7 cells (5×10^4 cells/well) were cultured in 5% CO_2 incubator at 37°C for 24 h in RPMI 1640 medium (containing 10% fetal calf serum, 100 U/ml penicillin, and 100 μl/ml streptomycin) in 96-well plates. The cells were divided into four groups (8 wells in each group): control group: cells were incubated in the absence of C-PC; He–Ne laser radiation group: cells received 2-min He–Ne laser radiation everyday in the absence of C-PC; C-PC group: cells were incubated in the presence of 80 μg/ml C-PC; C-PC + He–Ne laser radiation group: cells were incubated in the presence of 80 μg/ml C-PC for 2 h prior to 2-min He–Ne laser radiation. After 72 h of incubation, MCF-7 cells were ready for different studies. For MTT assay, 20 μl of MTT (5 mg/ml in PBS) was added to each well, and cells were incubated for an additional 4 h at 37°C and then scraped and centrifuged. The precipitate was dissolved in 100 μl of DMSO and the absorbance value was measured at 490 nm [29].

Determination of apoptotic characteristics of MCF-7 cells by electron microscopy

Cultured MCF-7 cells were scraped, harvested by centrifugation (200 *g*, 10 min, 4°C), resuspended, and fixed in 2.5% glutaraldehyde for 2 h. After being washed with PBS, the cells were post-fixed in 1.5% osmium tetroxide, dehydrated through graded alcohol, and embedded in Epon 812 for subsequent sectioning. The ultrathin sections were stained with uranyl acetate and lead citrate, placed on grids, and examined under transmission electron microscope.

Western blot analysis of caspase-9 expression

Cultured MCF-7 cells were washed with ice-cold PBS and gently lysed for 30 s in 80 μl ice-cold lyses buffer (250 mM sucrose, 1 mM EDTA, 0.05% digitonin, 25 mM Tris, pH 6.8, 1 mM dithiothrietol, 1 μg/ml aprotinin, 1 μg/ml pepstatin, 1 μg/ml leupeptin, 1 mM PMSF, 1 mM benzamidine). Lysates were centrifuged at 14,340 *g* at 4°C for 5 min. Supernatants were electrophoresed on a 15% polyacrylamide gel and fractionated proteins were transferred from gel onto PVDF membrane. Subsequently, the membrane was blocked with pH 7.4 PBS (containing 1% BSA) overnight, incubated with rabbit anti-human caspase-9 monoclonal antibody (1: 50) at 37°C for 1 h, washed with pH 7.4 PBS (containing 0.1% Tween-20) for 3 min (five times in total), and incubated with horseradish peroxidase-labeled goat anti-rabbit IgG (1:400) at 37°C for 1 h. Finally, the caspase-9 protein was detected by DAB coloration for 15 min.

Immunofluorescence measurement of cytochrome c release

Harvested MCF-7 cells were dropped on microscope slides and fixed in 95% alcohol for 5 min, and then incubated with FITC-goat anti-human cytochrome c McAb (1:50) at 37°C for 45 min. After being washed twice with PBS, the slides were observed under fluorescence microscope. Negative control was designed as PBS substituting for primary antibody. Positive cells were counted in five randomly chosen high power fields (×400), and the percentage of positive cells showing cytochrome c release was calculated.

Analysis of Bcl-2 expression by immunohistochemistry

Cultured MCF-7 cells were harvested, washed twice with PBS, dropped on microscope slides previously coated with 0.1% poly-lysine solution, and fixed at room temperature by 4% polyformadehyde/0.1 M PBS for 20–30 min. After

washed with distilled water, the slides were treated with 30% H_2O_2:methanol (1:50) at room temperature for 30 min and washed again. Then, the slides were incubated with blocking buffer followed by the biotinylated rabbit anti-human Bcl-2 monoclonal antibody (Boster, 1:100) and SABC. DAB was used for color development. Slides were observed under light microscope. Five high-power fields ($\times 400$) were randomly selected, and percentage of positive cells showing the reduction of Bcl-2 expression was calculated.

Statistical analysis

The results were expressed as mean $\pm$ SE. Data were obtained from three independent experiments. Student's *t*-test was used for comparison between means. The difference was considered statistically significant when $P < 0.05$. SPSS software was used.

Results

Determination of the tumor weight and tumor forming rate

When compared with the control group, both the tumor weight and tumor forming rate were lowered in C-PC group. However, both indexes were further reduced in C-PC + laser group ($P < 0.05$, **Fig. 1**). On the contrary, He–Ne laser was found to be of no significant effect on the tumor growth. These results illustrated that C-PC showed anti-tumor activity, and the combination of C-PC and He–Ne laser radiation could strikingly inhibit tumor formation.

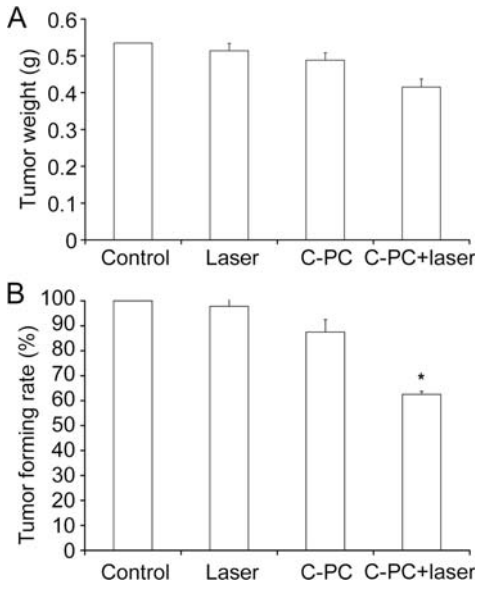

Figure 1 Effects of C-PC and He–Ne laser on tumor weight and tumor forming rate (A) Effects of C-PC and He–Ne laser on tumor weight. (B) Effects of C-PC and He–Ne laser on tumor forming rate. Tumor forming rate was significantly reduced in C-PC + laser group compared with the control group. *$P < 0.05$ vs control group.

Effects of C-PC and He–Ne laser on immune organs and immunocytes

Figure 2 demonstrated that C-PC could promote organs growth and proliferation of thymocytes and splenocytes of the mice with tumor. When compared with the control group, a significant increase in the numbers of thymocytes and splenocytes was found in C-PC group ($P < 0.05$). Nevertheless, the immunocyte proliferation was further increased when the cells were treated with C-PC and He–Ne laser radiation ($P < 0.01$). The results suggested that C-PC had immune-enhancing activity, which was especially enhanced in combination with laser radiation.

Effects of C-PC and He–Ne laser on the expressions of FAS, NF-κB, and P53 in tumor tissue

Positively stained cells in tumor tissue determined by immunohistochemistry showed brownish yellow color which mainly localized in cytomembrane and cytoplasm. As shown in **Fig. 3**, positive cells in C-PC group were

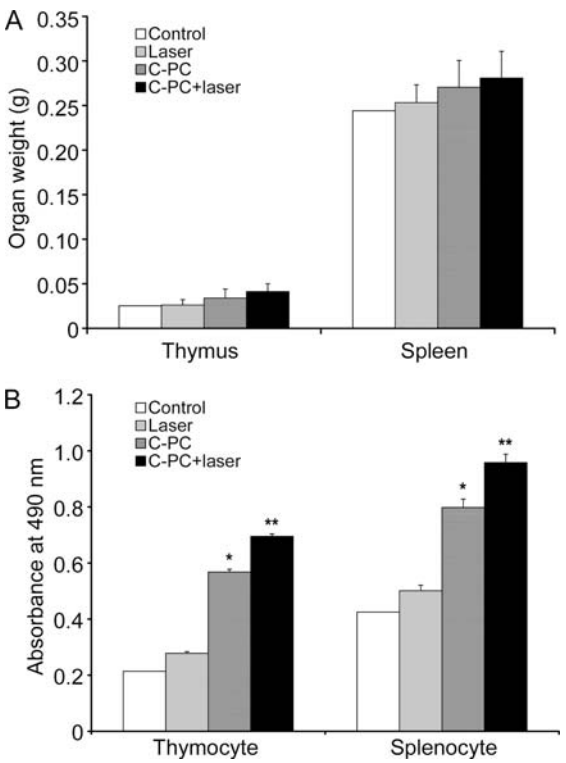

Figure 2 Determination of immune organs weight and immunocyte proliferation ability by MTT assay (A) Determination of immune organ weight. (B) Determination of immunocyte proliferation ability by MTT assay. C-PC could promote the proliferation of immunocytes (thymocytes and splenocytes) of the mice with tumor (*$P < 0.05$ compared with the control group). He–Ne laser radiation showed synergic effects when combined with C-PC (**$P < 0.01$).

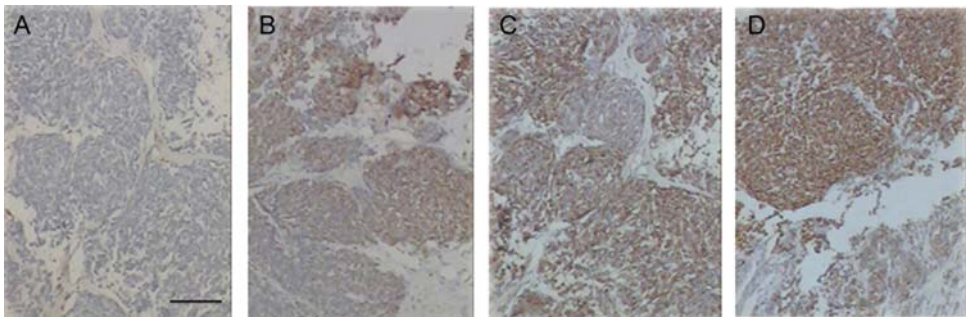

Figure 3 Effects of C-PC and He–Ne laser on Fas protein expression by immunohistochemical staining (A) Control group; (B) laser group; (*C*) C-PC group; (D) C-PC + laser group. Positively stained cells showed brownish yellow color which mainly localized in cytomembrane and cytoplasm. The positive cells in C-PC treatment group was dyed more fuscous than that in untreated control group, whereas the positive cells in C-PC + laser treatment group were much saturated than the other three groups. He–Ne laser radiation alone has no clear efficacy. Scale bar = 50 μm.

Table 1 Effects of C-PC and He–Ne laser on NF-κB and P53 expressions in the tumor tissue

Group (*n*)	NF-κB					P53				
	−	+	++	+++	Positive rate (%)	−	+	++	+++	Positive rate (%)
Control (16)	1	3	4	8	93.75	1	2	3	10	93.75
He-Ne laser (16)	1	5	4	6	93.75	1	4	2	9	93.75
C-PC (14)	3	6	3	2	70.00*	3	5	3	3	85.71*
C-PC + laser (10)	5	2	2	1	50.00**	4	4	1	1	60.00**

−, Negative; +, slightly positive; ++, moderately positive; +++, strongly positive. *n*, number of mice. *$P < 0.05$ vs control group. **$P < 0.01$ vs control group.

stained more fuscous than in the control group that was similar to He–Ne laser group, whereas positive cells in C-PC + laser group was most intensely stained. These results indicated that C-PC could promote the Fas expression of tumor tissue, and when combined with He–Ne laser, this effect was further enhanced.

Table 1 revealed that the positive rates of both NF-κB and P53 expressions in tumor tissue of C-PC group (70% and 85.71%, respectively) were lower than those in control group (both 93.75%) ($P < 0.05$), but higher than those of C-PC + He–Ne laser group (50 and 60%, respectively) ($P < 0.01$). Theses results suggested that C-PC could restrain the NF-κB and P53 expressions, and in the presence of He–Ne, the inhibitory effects were more distinct.

Influence of C-PC + He–Ne laser on *CD44* mRNA expression in tumor tissue

Synthesized CD44 oligonucleotide probes were applied to determine the expression of *CD44* mRNA. The results of *in situ* nucleic acid hybridization observed under light microscope showed that positive cells were stained brownish yellow, which mainly resided in cytomembrane and cytoplasm. **Figure 4** showed that the expression of *CD44* mRNA in tumor tissue in C-PC + laser radiation group was obviously less than those in either C-PC group or He–Ne laser group. He–Ne laser group and control showed similar *CD44* expression. These results suggested that C-PC treatment alone could suppress the *CD44* mRNA expression of tumor tissue and He–Ne laser illumination alone had no obvious effects. However, C-PC combined with He–Ne laser radiation could significantly decrease the expression of *CD44* mRNA.

Combination of C-PC and He–Ne laser inhibited the growth of MCF-7 cells *in vitro*

In order to determine the effects of C-PC and He–Ne laser on the growth of MCF-7 cells *in vitro*, MTT assay was adopted. The results demonstrated that the number of MCF-7 cells survived in C-PC group was obviously fewer than that of control group or that of He–Ne laser group ($P < 0.05$). However, if the cells were treated with C-PC + He–Ne laser radiation, the number of survived MCF-7 cells was further decreased ($P < 0.01$, **Fig. 5**). So, C-PC had inhibitory effect against the proliferation of MCF-7 cells *in vitro*, and this inhibitory activity could be enhanced by He–Ne laser radiation.

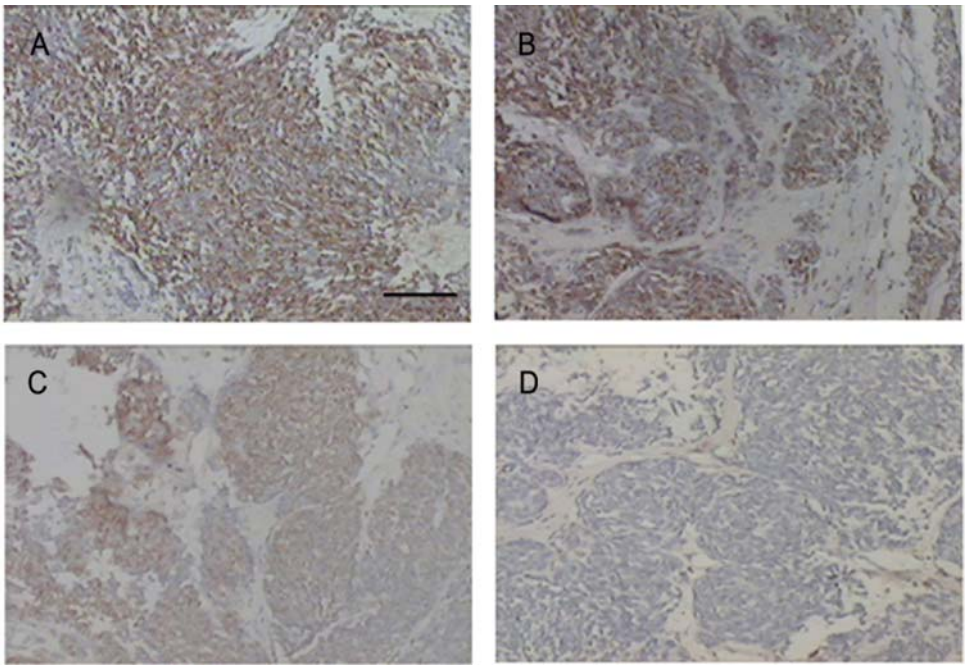

Figure 4 Screening *CD44* mRNA expression by *in situ* hybridization (A) Control group; (B) laser group; (C) C-PC group; (D) C-PC + laser group. Positive cells were stained brownish yellow, which mainly resided in cytomembrane and cytoplasm. The expression quantities of *CD44* mRNA in tumor tissue in C-PC + laser radiation group were obviously lower than those in either C-PC group or He–Ne laser group in which CD44 expression quantities resembled those in control group. Scale bar = 50 μm.

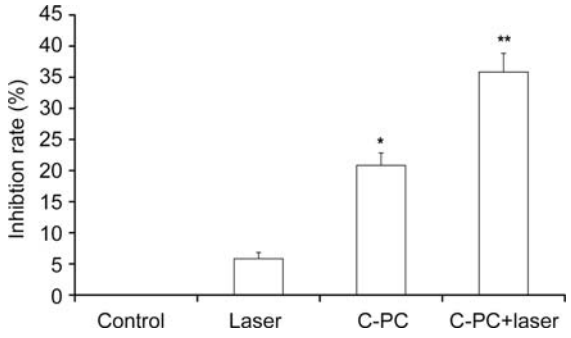

Figure 5 MCF-7 cell viability determined by MTT assay Both C-PC group ($*P < 0.05$ compared with control group) and He–Ne laser group could inhibit MCF-7 cell proliferation. However, if the cells were treated with C-PC + He–Ne laser radiation, proliferation of MCF-7 cells were further inhibited ($**P < 0.01$).

Electron microscope observation of MCF-7 cell apoptosis

To judge whether the anti-tumor activity of C-PC and He–Ne laser was associated with apoptosis, we further discerned the ultrastructural changes of MCF-7 cells by transmission electron microscopy. Results revealed the presence of a series of morphological changes such as loss of microvilli and blebbing of cell membrane in C-PC group and chromatin condensation into dense granules or blocks in C-PC + laser group, all of which were characteristics of cells undergoing apoptosis. On the contrary, untreated control cells exhibited normal morphology and no sign of apoptosis appeared (**Fig. 6**). These results further confirmed that C-PC together with He–Ne radiation could induce MCF-7 cells death by apoptosis.

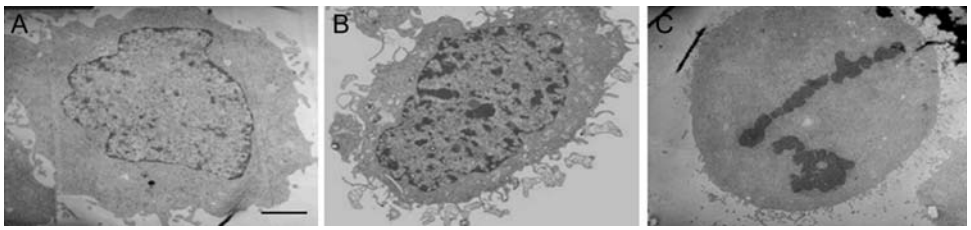

Figure 6 Electron micrographs of MCF-7 cells (A) Untreated control cells which showed normal morphology and no sign of apoptosis appeared. (B) MCF-7 cells treated with C-PC. The cells showed apoptotic morphology including chromatin condensation into dense granules or blocks. (C) MCF-7 cells exposed to C-PC and He–Ne laser irradiation treatments. The cells showed loss of microvilli and blebbing of cell membrane which were characteristics of cells undergoing apoptosis. These results further confirmed that C-PC together with He–Ne radiation could induce MCF-7 cells death by apoptosis. Scale bar = 3 μm.

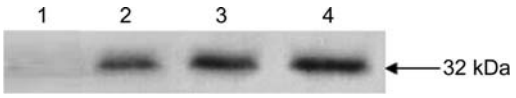

Figure 7 Western blot analysis of caspase-9 expression MCF-7 cells were analyzed by 15% SDS–PAGE, and after electrophoresis, proteins on the gel were transferred to nitrocellulose membrane and probed with mouse anti-caspase-9 monoclonal antibody. Lane 1: control group; lane 2: He–Ne laser group; lane 3: C-PC group; lane 4: C-PC + He–Ne laser group.

Effects of C-PC and He–Ne laser on the caspase-9 expression of MCF-7 cells *in vitro*

In the present study, western blot analysis was used to measure the caspase-9 expression. As depicted in **Fig. 7**, caspase-9 was almost not detectable in the cytoplasm in untreated control cells (lane 1), whereas after He–Ne laser radiation at MCF-7 cells, caspase-9 expression was increased (lane 2). C-PC alone (lane 3) or in combination with He–Ne laser (lane 4) could further increase caspase-9 activities in MCF-7 cells.

Detection of cytochrome c release

The release of cytochrome c, one of the most important respiratory-chain proteins, from the mitochondria into the cytosol is the hallmark of cells passing through apoptosis. To specify the molecular basis of apoptosis, the release of cytochrome c into the cytosol was screened in MCF-7 cells by immunofluorescence analysis. The fluorescence intensity in cytosol in C-PC group, which represented the quantities of cytochrome c, was higher than those in control group or in He–Ne laser group. When the MCF-7 cells were treated with C-PC + He–Ne laser, the fluorescence intensity was clearly elevated (**Fig. 8**). The percentage of cells showing the release of cytochrome c was 40.6% in C-PC group and 65.2% in PDT group. However, in control group and He–Ne laser group, the data were 6.5% and 11.1%, respectively.

Effects of C-PC and He–Ne laser on Bcl-2 protein expression

Bcl-2 residing in mitochondria is novel among proto-oncogenes and shows the unique functional role of blocking apoptosis. Many researches argue that Bcl-2 provided a distinct survival signal to cells and may contribute to neoplasia. Positively stained cells showed brownish yellow color. As shown in **Fig. 9**, MCF-7 cells in C-PC group were stained more slightly than in the control group, whereas the cells in C-PC + laser group were most slightly stained. The percentage of cells showing the reduction of Bcl-2 protein synthesis was 39.7% in C-PC group and 68.4% in PDT group. However, in control group and He–Ne laser group, the data were 7.4% and 10.3%, respectively. These results suggested that untreated cells expressed higher levels of Bcl-2 protein, which was down-regulated in C-PC treated cells. With the help of He–Ne laser radiation, C-PC could further down-regulate the production of the Bcl-2 protein.

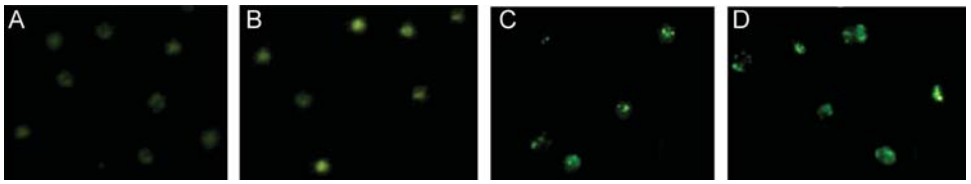

Figure 8 Immunofluorescence measurement of cytochrome c release (×400) (A) Control group; (B) He–Ne laser group; (C) C-PC group; (D) C-PC + He–Ne laser group. From Groups A to D, the fluorescence intensity was gradually strengthened which represented release quantities of cytochrome c were increased. The quantities of cytochrome c in cytosol in the MCF-7 cells of C-PC group was higher than those in untreated control group or in He–Ne laser group. Combination of C-PC and He–Ne laser treatment obviously increase cytochrome c release as shown by the fluorescence intensity.

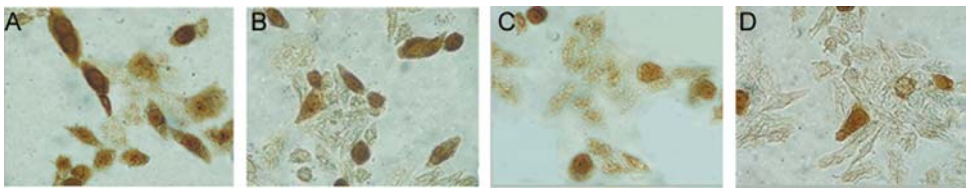

Figure 9 Immunohistochemistry determining the effects of C-PC + He–Ne laser on Bcl-2 expression (×400) (A) Control group; (B) He–Ne laser group; (C) C-PC group; (D) C-PC + He–Ne laser group. Positive cells took on brownish yellow color. MCF-7 cells in C-PC group were stained more slightly than in the control group, whereas the cells in C-PC + laser group were most slightly stained. These results indicated untreated cells expressed higher levels of Bcl-2 protein which was down-regulated in C-PC treated cells. In combination with He–Ne laser radiation, C-PC could further down-regulate the expression of the Bcl-2 protein in MCF-7 cells.

Discussion

In present study, a natural substance, C-PC, isolated from *S. platensis*, was investigated for its potential as a new promising photosensitizer in PDT. The functional mechanisms of C-PC-mediated PDT in inducing MCF-7 cell apoptosis were explored both *in vivo* and *in vitro*.

The mice tumor model was successfully established by subcutaneous injection of MCF-7 cells. He–Ne laser radiation and C-PC treatment were applied for the investigation of their possible therapeutic effects and the functional mechanisms. The results suggested that C-PC had an anti-tumor activity, and if in combination with He–Ne laser treatment, the effects were further heightened.

The mechanism of tumor destruction by PDT incorporates a variety of events leading to the inactivation of tumor cells. Once generated by PDT, it is conceivable that these immune cells can be engaged in additional eradication of disseminated and/or metastatic lesions of the same cancer [30]. A number of immunotherapy regimens have already been proven effective in enhancing the curative effect of PDT with various animal tumor models. It has been proved that PDT could induce non-specific and specific immune reactions which might improve PDT-mediated anti-tumor efficacy [31–33]. In the present study, the effects of C-PC in combination with He–Ne laser on immune organs and immunocytes were investigated. The data illustrated that C-PC had an immune enhancing activities, which were increased when applied together with He–Ne laser.

The occurrence of apoptosis as a mechanism of PDT-mediated cell death has previously been demonstrated both *in vitro* [34,35] and *in vivo* [36]. For example, phthalocyanine-mediated PDT has been shown previously to induce apoptosis and G_0/G_1 cell cycle arrest in A431 human epidermoid carcinoma cells [37]. In the present study, immunohistochemistry analysis showed that C-PC treatment together with He–Ne laser radiation, could enhance pro-apoptotic Fas protein expression (**Fig. 3**), meanwhile held back the expressions of anti-apoptotic NF-κB, P53 proteins, and *CD44* mRNA (**Table 1** and **Fig. 4**). These results confirmed C-PC was an ideal photosensitizer, which accumulates in tumor tissue and attracts He–Ne laser to target at the cancer tissue. Consequently, C-PC induced the activation of pro-apoptotic genes and down-regulation of anti-apoptotic genes expression, and then facilitated the transduction of tumor apoptosis signals that resulted in the apoptosis of MCF-7 cells *in vivo*.

In order to comprehensively reveal the functional mechanism of C-PC-mediated PDT in MCF-7 cells, *in vitro* studies using MCF-7 cells were carried out. MTT assay was adopted to determine the effects of C-PC cooperating with He–Ne laser on the growth of MCF-7 cells. The results showed that C-PC treatment combined with He–Ne laser radiation could significantly inhibit MCF-7 cell growth (**Fig. 5**).

Apoptosis is a specific mode of cell death recognized by a characteristic pattern of morphological, biochemical, and molecular changes [38–40]. The present study demonstrated the cultured MCF-7 cells treated by C-PC together with He–Ne laser took on remarkably morphological changes like cell shrinkage, formation of membrane blebs, nuclear and cytoplasmic condensation, and micronuclei, as observed under transmission electron microscope (**Fig. 6**).

As is well known, caspase-9 plays a vital role in virtually apoptotic signaling pathways, so we analyzed the caspase-9 activation in MCF-7 cells treated with C-PC + He–Ne laser. Results showed that caspase-9 was activated in MCF-7 cells treated with C-PC and its activity was apparently elevated in C-PC + He–Ne laser group (**Fig. 7**). Caspase-9 was an initiator of apoptosis, and it was regulated by Fas/tumor necrosis factor receptor-1 (TNF-R1) and TNF-related apoptosis-inducing ligand (TRAIL). When Fas/TNF-R1 combined with ligand, caspase-9 would be activated. The present data suggested that C-PC-mediated PDT induced caspase-dependent apoptosis.

One of the major apoptotic pathways is activated by the release of apoptotic protein, cytochrome c, from mitochondria into the cytosol. To specify the molecular basis of apoptosis, the release of cytochrome c into the cytosol was measured in MCF-7 cells by immunofluorescence analysis. According to the variation of fluorescence intensity of cytochrome c in cytoplasm (**Fig. 8**), it was found C-PC treatment could induce cytochrome c release, and this inducing effect can be enhanced with the assistance of the He–Ne laser radiation.

Plenty of evidences suggest that blocks in the process of apoptosis may be closely associated with carcinogenesis and that many cancer cells have defensive machinery for self-destruction [41]. The photosensitizer PC4, a silicon phthalocyanine used in PDT, could induce translocation of the pro-apoptotic Bax from the cytosol to the mitochondria in human breast cancer MCF-7cs cells [42]. Bcl-2 has emerged as a new type of proto-oncogene interfered with apoptosis independent of promoting cell division [43]. He–Ne laser has little effect on anti-apoptotic Bcl-2 protein expression in MCF-7 cells. However, when a combination of C-PC and He–Ne laser was applied, Bcl-2 protein expression levels were down-regulated (**Fig. 9**), which might be responsible for C-PC-mediated PDT induced apoptosis in MCF-7 cells through the continuous transduction of tumoral apoptosis signals.

In a word, C-PC-mediated PDT was approved as a potential therapy for cancer. The functional mechanism may be that, acting as a good photosensitizer, C-PC is accumulated in tumor tissue, and He–Ne light delivery can be targeted to the tumor tissue, and the combination has

provided an effective tumor therapy with efficient cytotoxicity and limited damage to the surrounding normal tissue. C-PC-mediated PDT was found to activate immune system, including amplification of leukocytes activity after PDT. In addition, C-PC-mediated PDT was able to cause an apoptotic response in cancer cells, which explained the extensive efficacy of PDT. Moreover, C-PC-mediated PDT could preferably induce the activation of pro-apoptotic Fas genes and down-regulation of anti-apoptotic protein expression such as Bcl-2, NF-κB, P53, and *CD44* mRNA. When Fas binds to its ligand, caspase-9 would be activated. Cytochrome c is released into cytocol and forms the apoptotic complex with caspase-9, apoptosis protease-activating factor, and dATP, which in turn activates caspase-9. Caspases activation facilitates the transduction of tumoral apoptosis signals, resulting in the cleavage of cellular substrates and eventually leading to apoptosis of MCF-7 cells.

The present study put forward a new idea for the molecular mechanism of C-PC-mediated PDT and a theoretic basis. Since C-PC is a natural pigment and a component of edible *Spirulina* extracts, having no toxic side effects, it might become a good substitute to highly toxic conventional photosensitizers or chemotherapeutic anticancer drugs in the future. Furthermore, C-PC mediated-PDT technique is easy, inexpensive, and of short duration, so it is useful to develop a new way for the treatment of cancer.

Funding

This work was supported by grants from the Science Research Award Foundation of Middle-age and Young Scientist of Shandong Province (No. 2007BS03016 to B.L.), the National Natural Science Foundation of China (No. 30170893 to M.G.) and Science Research Development Foundation of Shandong Province Education Department (No. J07YE16-2).

References

1 Brown SB, Brown EA and Walker I. The present and future role of photodynamic therapy in cancer treatment. Lancet Oncol 2004, 5: 497–508.
2 Nyst HJ, Tan IB, Stewart FA and Balm AJ. Is photodynamic therapy a good alternative to surgery and radiotherapy in the treatment of head and neck cancer? Photodiagnosis Photodyn Ther 2009, 6: 3–11.
3 Sharman WM, Allen CM and van Lier JE. Photodynamic therapeutics: basic principles and clinical applications. Drug Discov Today 1999, 4: 507–517.
4 Stapleton M and Rhodes LE. Photosensitizers for photodynamic therapy of cutaneous disease. J Dermatol Treat 2003, 14: 107–112.
5 Morcos NC, Berns M and Henry WL. Phycocyanin: laser activation, cytotoxic effects, and uptake in human atherosclerotic plaque. Lasers Surg Med 1988, 8: 10–17.
6 Vadiraja BB, Gaikwad NW and Madyastha KM. Hepatoprotective effect of C-phycocyanin: protection for carbon tetrachloride and R-(+)-pulegone-mediated hepatotoxicty in rats. Biochem Biophys Res Commun 1998, 249: 428–431.
7 Romay C and Gonzalez R. Phycocyanin is an antioxidant protector of human erythrocytes against lysis by peroxyl radicals. J Pharm Pharmacol 2000, 52: 367–368.
8 Bhat VB and Madyastha KM. C-phycocyanin: a potent peroxyl radical scavenger *in vivo* and *in vitro*. Biochem Biophys Res Commun 2000, 275: 20–25.
9 Romay C, Ledon N and Gonzalez R. Further studies on anti-inflammatory activity of phycocyanin in some animal models of inflammation. Inflamm Res 1998, 47: 334–338.
10 Hu XM. Medical physics. (5th edn). Beijing: People's Medical Publishing House, 2001, 351–352.
11 Qin RJ. Medical physics. (3rd edn). Guilin: GuangXi Normal University Press, 2002, 131–132.
12 Stadler I, Lanzafame RJ, Oskoui P, Zhang RY, Coleman J and Whittaker M. Alteration of skin temperature during low-level laser irradiation at 830 nm in a mouse model. Photomed Laser Surg 2004, 22: 227–231.
13 Rochkind S and Ouaknine GE. New trend in neuoscience: low-power laser effect on peripheral and central nervous system (basic science preclinical and clinical studies). Neurol Res 1992, 14: 2–11.
14 Pogrel MH, Chen JW and Zhang K. Effects of low-energy gallium-alrminum-arsenide laser irradiation on cultured fibroblasts and keratinocytes. Lasers Surg Med 1997, 20: 426–432.
15 Ben-Dov N, Shefer G, Irintchev A, Oron U and Halevy O. Low energy laser irradiation affects satellite cell proliferation and differentiation in vitro. Biochim Biophys Acta 1999, 14: 372–380.
16 Grossman N, Schneid N, Reuveni H, Halevy S and Lubart R. 780 nm low power diode laser irradiation stimulates proliferation of keratinocyte cultures: involvement of reactive oxygen species. Lasers Surg Med 1998, 22: 212–218.
17 Pessoa ES, Melhado RM, Theodoro LH and Garcia VG. A histologic assessment of the influence of low-intensity laser therapy on wound healing in steroid-treated animals. Photomed Laser Surg 2004, 22: 199–204.
18 Brosseau L, Welch V, Wells G, DeBie R, Gam A, Harman K and Morin M, *et al*. Low level laser therapy (Classes I, II and III) for treating osteoarthritis. Cochrane Database Syst Rev 2004, 3: CD002046.
19 Kans JS, Hutschenreiter T, Haina D and Waidelich W. Effect of low-power density laser radiation on healing of open skin wounds in rats. Arch Surg 1981, 116: 293–296.
20 Hrnjak M, Kulijic-Kapulica N, Budisin A and Giser A. Stimulatory effect of low-power density He–Ne laser radiation on human fibroblasts *in vitro*. Vojnosanit Pregl 1995, 52: 539–546.
21 Monteforte P, Baratto L, Molfetta L and Rovetta G. Low-power laser in osteoarthritis of the cervical spine. Int J Tissue React 2003, 25: 131–136.
22 Ohta A, Abergel RP and Uitto J. Laser modulation of human immune system, inhibition lymphocyte proliferation by a gallium-arsenide laser energy. Lasers Surg Med 1987, 7: 199–201.
23 Karu T. Photobiology of low-power laser effects. Health Phys 1989, 56: 691–704.
24 Fukutomi H, Kawakita I and Nakahara A. Endoscopic diagnosis and treatment of gastric cancer by laser beam. Laser Endoscopy 1981, 20: 26.
25 Overholt BF, Danjehpour M and Haydek JM. Photodynamic therapy for Barrett's esophagus: follow-up in 100 patients. Gastrointest Endosc 1999, 49: 1–7.
26 Etienne J, Dorme N, Bourg-Heckly G, Raimbert P and Flijou JF. Photodynamic therapy with green light and m-tetrahydroxyphenyl chlorin for intramucosal adenocarcinoma and high-grade dysplasia in Barrett's esophagus. Gastrointest Endosc 2004, 59: 880–889.
27 Li B, Zhang X, Gao M and Chu X. Effects of CD59 on antitumoral activities of phycocyanin from *Spirulina platensis.*. Biomed Pharmacother 2005, 59: 551–560.

28 Korbelik M and Cecic I. Complement activation cascade and its regulation: relevance for the response of solid tumors to photodynamic therapy. J Photochem Photobio B 2008, 93: 53–59.
29 Kwitniewski M, Juzeniene A, Ma LW, Glosnicka R, Graczyk A and Moan J. Diamino acid derivatives of PpIX as potential photosensitizers for photodynamic therapy of squamous cell carcinoma and prostate cancer: *in vitro* studies. J Photochem Photobio B 2009, 94: 214–222.
30 He RZ. Pathology. 4th edn. Beijing: People's Medical Publishing House, 2003, 128–129.
31 Huang HF, Chen YZ, Wu Y, Li NN and Chen P. Efficacy of ZnPcS2P2 photodynamic therapy solely or with tumor vaccines on mouse tumor models. Photodiagnosis Photodyn Ther 2007, 4: 100–105.
32 Gray J and Fullarton G. The current role of photodynamic therapy in oesophageal dysplasia and cancer. Photodiagnosis Photodyn Ther 2007, 4: 151–159.
33 Castano AP, Mroz P and Hamblin MR. Photodynamic therapy and anti-tumor immunity. Nat Rev Cancer 2006, 6: 535–545.
34 Usuda J, Chiu SM, Murphy ES, Lam M, Nieminen AL and Oleinick NL. Domain-dependent photodamage to Bcl-2. A membrane anchorage region is needed to form the target of phthalocyanine photosensitization. J Biol Chem 2003, 278: 2021–2029.
35 Choi SE, Sohn S, Cho JW, Shin EA, Song PS and Kang Y. 9-Hydroxypheophorbide alpha-induced apoptotic death of MCF-7 breast cancer cells is mediated by c-Jun N-terminal kinase activation. J Photochem Photobiol B 2004, 73: 101–107.
36 Zhou C, Shunji C, Jinsheng D, Junlin L, Jori G and Milanesi C. Apoptosis of mouse MS-2 fibrosarcoma cells induced by photodynamic therapy with Zn (II)-Phthalocyanine. J Photochem Photobiol B 1996, 33: 219–223.
37 Ahmad N, Feyes DK, Agarwal R and Mukhtar H. Photodynamic therapy results in induction of WAF1/CIP1/p21 leading to cell cycle arrest and apoptosis. Proc Natl Acad Sci USA 1998, 95: 6977–6982.
38 Kuželová K, Grebenová D, Pluskalová M, Marinov I and Hrkal Z. Early apoptotic features of K562 cell death induced by 5-aminolaevulinic acid-based photodynamic therapy. J Photochem Photobiol B 2004, 73: 67–78.
39 Wyld L, Reed MW and Brown NJ. Differential cell death response to photodynamic therapy is dependent on dose and cell type. Br J Cancer 2001, 84: 1384–1386.
40 Dolmans DEJGJ, Fukumura D and Jain RK. Photodynamic therapy for cancer. Nat Rev Cancer 2003, 3: 380–387.
41 Tseng CJ, Wang YJ, Liang YC, Jeng JH, Lee WS, Lin JK and Chen CH, *et al*. Microtubule damaging agents induce apoptosis in HL 60 cells and G2/M cell cycle arrest in HT 29 cells. Toxicology 2002, 175: 123–142.
42 Haywood-Small SL, Vernon DI, Griffiths J, Schofield J and Brown SB. Phthalocyanine-mediated photodynamic therapy induces cell death and a G_0/G_1 cell cycle arrest in cervical cancer cells. Biochem Biophys Res Commun 2006, 339: 569–576.
43 Grobholz R, Zentgraf H, Kohrmann KU and Bleyl U. Bax, Bcl-2, Fas and FasL antigen expression in human seminoma: correlation with the apoptotic index. APMIS 2002, 110: 724–732.